Spline interpolation as a way of mapping pollen emission sources

Article *in* Aerobiologia · December 2021

DOI: 10.1007/s10453-021-09707-6

4 authors, including:

V. Rodinkova
National Pirogov Memorial Medical University
72 PUBLICATIONS **485** CITATIONS
SEE PROFILE

Vitalii Mokin
Vinnytsia National Technical University
78 PUBLICATIONS **38** CITATIONS
SEE PROFILE

Tetiana Vuzh
National Pirogov Memorial Medical University
8 PUBLICATIONS **5** CITATIONS
SEE PROFILE

SPLINE INTERPOLATION AS A WAY OF MAPPING POLLEN EMISSION SOURCES

V. Rodinkova[1], V. Mokin[2], T. Vuzh[2], M. Dratovanyj[2]
1 – National Pirogov Memorial Medical University, Vinnytsya; Vinnytsia, Ukraine
2 – Vinnytsia National Technical University; Vinnytsia, Ukraine

Corresponding author: Victoria Rodinkova, vikarodi@gmail.com, +380505499656
Victoria Rodinkova https://orcid.org/0000-0003-0741-1104
Vitalii Mokin http://orcid.org/0000-0003-1946-0202

Abstract: The article develops a new method of spatiotemporal modelling of possible locations of ragweed areas and estimation of pollen emission intensity of these areas. The method uses spline approximation with automatic computations of typical pollen production models in the R language. It applies a number of approaches eliminating the uncertainty of various parameters that should be taken into consideration for this modelling. The authors have consolidated some experimental data on the amount of *Ambrosia* pollen in the air depending on environmental conditions, and found some new possible ragweed pollen sources on the territory of the city of Vinnytsia and the adjacent villages.

The study used spline approximation of the first (lines) and second (parabolas) orders were applied. Data of bi-hourly pollen concentrations obtained at the pollen monitoring site of National Pirogov Memorial Medical University (Vinnytsia).

To perform the approximation, wind speed, wind direction and relative humidity were taken into the consideration. The authors used the polar coordinate system to formalize the problem.

PRA Finder computer program was developed, which has been successfully tested on real data and for which a certificate of copyright registration has been obtained in Ukraine.

As a result of the method application, the known areas were corroborated and new possible plots were revealed. The comparison of the forecasted areas for 2014 with the actual ones showed a close match.

However, it should be taken into consideration that the proposed method is viable only when applied under the condition that the wind velocity does not exceed 4 m/sec and the relative humidity is between 20 % and 90 %.

Key words: ragweed inventories, spline interpolation, spatiotemporal modelling, task uncertainty, R language

Declarations

Funding
The study was supported by the statutory funds of the Scientific Research Center of the National Pirogov Memorial Medical University, Vinnytsya and by the Department of Systems Analysis, Computer Monitoring and Engineering Graphics of the Vinnytsia National Technical University.

Conflicts of interest/Competing interests
Authors declare neither conflict of interest nor competing interests

Availability of data and material
Authors declare that all the data used for this study was either the intellectual property of the authors or obtained from the avaliable sources.

Authors' contributions (optional: please review the submission guidelines from the journal whether statements are mandatory)
V. Rodinkova – pollen count data, Manuscript concept, editing, reviewing
V. Mokin – spline interpolation application, methodology, its step-by-step explanation
T. Vuzh – writing the first draft of the Manuscript, editing, reviewing, investigation and mapping of areas, infested by ragweed
M. Dratovanyj – R language programming, performance of simulation

1 Introduction

The last few years were associated with an increased interest of the public on accurate and prompt prediction of pollen levels in the atmosphere. And the most forecasted taxa were *Betula*, *Poaceae* and *Ambrosia* (Maya-Manzano J.M. et. al., 2020). Their popularity is associated with the significant impact of these pollen types on the human health. In particular, active distribution of ragweed in Ukraine, which is a well-known area of ragweed (*Ambrosia spp.*) in Europe (Montagnani et. al., 2017), promoted high levels of sensitization of Ukrainian population to the pollen of this plant. Currently, according to the data of multicomponent molecular allergy diagnostics, 80 % of the 8016 tested individuals with pollen allergy are sensitized to *Ambrosia* pollen in the Ukrainian areas with the most rapid spread of ragweed. An average sensitization rate exceeds 40 % of tested individuals all over Ukraine (Rodinkova et. al, 2019). During the previous decades, an explosive spread of ragweed was observed in our country, especially in Southern, Southeastern and Central regions (Rodinkova et. al., 2018).

Thus, the importance of the ragweed allergy in Ukraine cannot be overestimated. What is more, *Ambrosia* spread is continuing in our country now (Hamaoui-Laguel et al. 2015; Matyasovszky et. al, 2018). However, all the areas of this plant, especially new ones, may be unknown. This decreases the efficacy of the ragweed eradication and increases the health effects of ragweed pollen, including the pollen which is associated with long distance transport. In addition, accurate information about the pollen sources helps to either prevent or decrease contact of patients with this pollen (Mokin, 2007; Prank et.al, 2013).

While on site observations and mapping of new ragweed areas may be conducted with a delay, it is important to look for methods which may help to determine and model the spatial spread of *Ambrosia* plants. The problem of modelling the process of production and spread of *Ambrosia* pollen is investigated by many scientists all over the world, including Europe (Allergenic Pollen, review, 2013; Letty A De Weger et. al, 2016; Stepalska D et. al., 2020). The examples of successful modelling of pollen spread —

namely, of ragweed — include those done by SILAM and Cosmo Art models (Prank et.al, 2013; Zink et. al, 2012). Another example of estimation of ragweed pollen emission and dispersion is an application of a RegCM-pollen model (L. Liu et. al, 2015).

In contrast with the known models, which are mostly used at the continental and large regional scales (Sikoparija, B. et. al., 2016; Sikoparija, B. et. al., 2017;), the current study aimed to determine possible emission sources of ragweed at the regional and local scales.

Therefore, **the aim** of our study was to create a localised model, which is able to determine possible ragweed pollen sources in the city of Vinnytsia and the adjacent villages, using the spline interpolation based on the data of bihourly pollen count.

2 Materials and methods

Sampler location and sampling methodology

Pollen sampling was made employing Burkard pollen and spore trap of Hirst type (1952) located at the 49°13'39.9"N and 28°26'41.6"E on the roof of the chemical building of the National Pirogov Memorial Medical University, Vinnytsya, Ukraine. The altitude of pollen trap was 25 m above the ground. Sampler pumped air with a speed of `10 litre per minute. This speed was controlled by the rotameter, provided by the Burkard Company.

A 345 mm-long strip of Melinex tape was fixed onto a clock-controlled drum that made a complete revolution in one week. Before sampling, the Melinex tape was coated with an adhesive (a solution of pure silicon and carbon tetrachloride). After the tape was removed from the drum, it was cut into seven even pieces representing the seven days of sampling. Each daily segment was made into a microscope sample that was mounted on a slide using glycerin and gelatin mixture. For better pollen identification the samples were stained with the same solution containing basic fuchsin.

Pollen count was performed bihourly using the method of 12 vertical transects under magnification of 400 × using a Zeiss Axioscop microscope (Germany) so that the area of analysed surface was 11.25%, which meets the minimum requirements to pollen monitoring (Galán et. al 2014).

Pollen count was recalculated into pollen grains' concentration per cubic meter of ambient air, using the relevant formula. The latter took into account the sampled and analysed areas of the slide, volume of the air pumped through the orifice of the sampler per minute and per day. *Ambrosia* pollen concentrations for the years 2013 and 2014 were used for further analysis.

Area of sampling and its main climatic conditions

The trap was located in the highly urbanized downtown area and was surrounded by a compact urban development that consisted mainly of multi-storey buildings. Other buildings did not obscure the trap and generally were of either the same height or lower. Except for the multi-storey buildings and, to a lesser extent, the individual households, the area around the trap included the low-rise buildings and townhouses of the suburbs. The city is surrounded by agricultural fields and forests.

Generally, the Vinnytsia region is located in the temperate zone and has forest-steppe landscapes. The climate of the Vinnytsia region is moderately continental, characterized by long, warm and fairly humid summers, early spring, dry autumn, moderate frost and heavy snow cover in winter. The coldest month is January and the warmest month is July. Average amplitudes of temperature fluctuations during the year do not exceed 25°C. The highest temperatures are observed in July-August. The average annual amount of precipitation in the region is 440-590 mm. The winter months are the least wet, they account for 25% of annual precipitation. The beginning of spring corresponds with the transition of the daily temperature through the 0°C and occurs most often in the second fortnight of March. Spring lasts for about two months. Summer runs from the second fortnight of May to the first fortnight of September. The daytime temperatures in May are + 18 ... + 20°C, in July – + 21 ... + 25°C. The highest levels of precipitation, mainly showers, occur in this season. The number of days with precipitation decreases gradually, when autumn approaches. Autumn begins with the downward transition of the average daily temperature through + 10° C. The onset of autumn occurs in the first fortnight of October. A characteristic feature of the autumn in Vinnytsia is the occurrence of warm sunny days. The autumn ends at the end of November, when the average daily temperature drops below 0°C (Vinnytsia Regional State Administration, 2017).

Meteorological data and its processing

The official meteorological data of relative humidity, wind speed and velocity was obtained from the meteorological station of Vinnytsia. The meteorological data were recalculated in the same bi-hourly mode to match the provided pollen data. Given the various uncertainties of a number of parameters, the change of humidity with height was not taken into account. The calculations were performed in the first approximation.

Spline interpolation' methodology argumentation and description

To perform the current study, the authors have also consolidated some existing experimental data about the concentration of *Ambrosia* pollen in the air in relation to relative humidity (Martin et al., 2010). This data provided typical curves of the hourly amount of *Ambrosia* pollen in the air depending on different values of the relative humidity (RH) ranging from 20% to 90%. This information is characteristic of a range of latitudes in Europe and it can also be used as typical solution curves for the monitoring station in Vinnytsia.

The data provided by Martin et. al, 2010, have been recalculated for a 2-hour interval (Fig.1). It was done because the calculation of the experimental data described by Martin at al., 2010 was performed every hour, while for the Vinnytsia air monitoring station only bi-hourly pollen data are available.

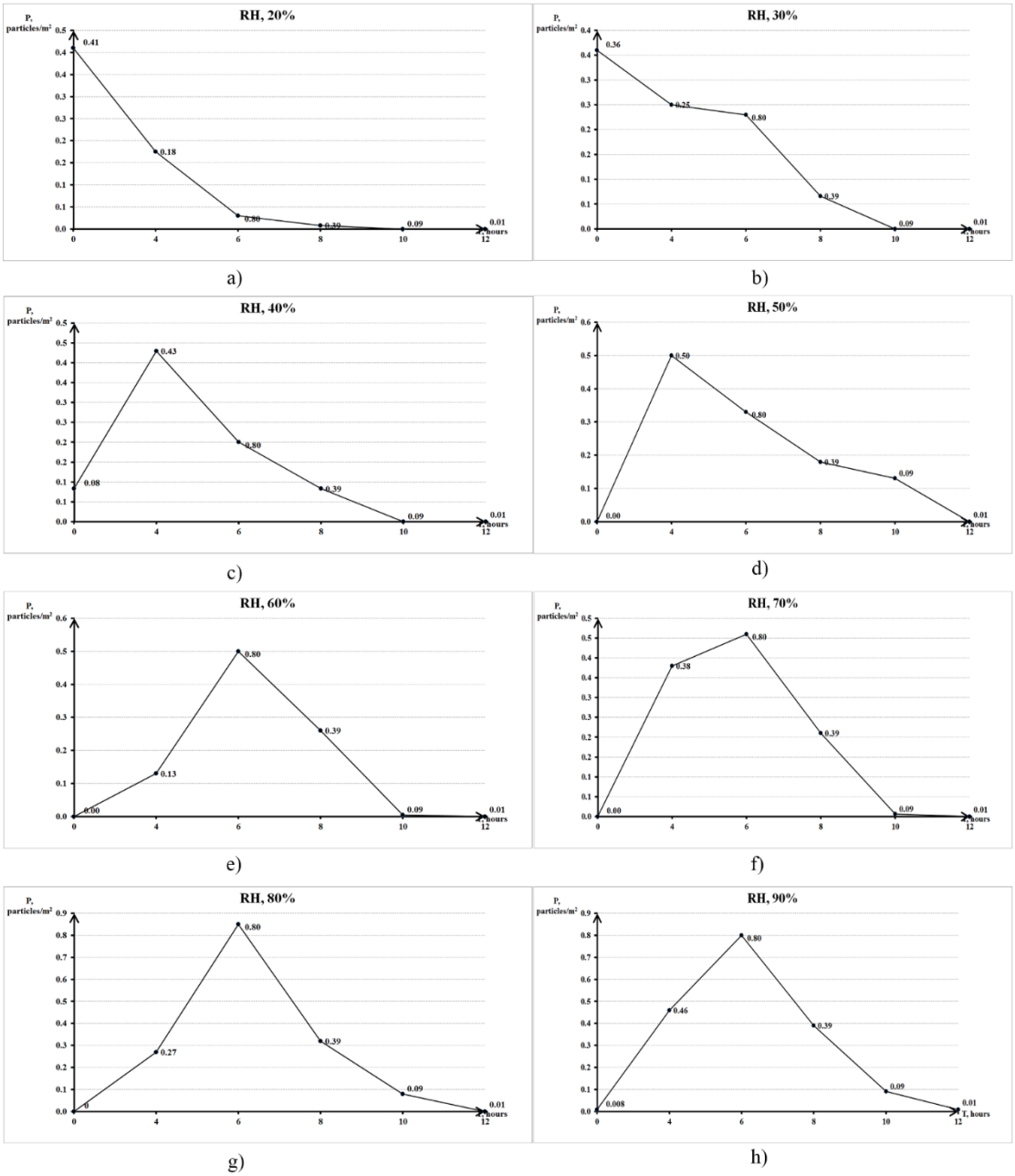

Fig.1. Typical curves of the amount of *Ambrosia* pollen in the air ***P*** calculated for values at 2-hour intervals depending on different values of the relative humidity ***RH*** from 20% to 90% (Martin et. al., 2010)

The spline interpolation method was used to achieve the aim of the study. However, the analysis of possible approaches to analytical description of these typical curves revealed that the researchers did not have enough data (the number of non-zero values is from 3 to 6) to identify complex analytical functions. In addition, the approximation employing the quasiconvex function, the Gaussian function, logistic, trigonometric and polynomial functions with a minimum number of parameters did not produce the desired precision or monotonicity. That is why we opted to use spline approximation of the first (lines) and second (parabolas) orders. The values of these curves y_i, $i= 1, 2, \ldots, N$ were used as a "mask" that is supposed to be "put up" to each real graph showing the values of experimental data about the amount of pollen p_i; the "mask" then should just be adjusted vertically so that its peak is aligned with the daily peak value.

$$p_i = Iy_i, i = \overline{1, N} \quad (1)$$

where

p_i is the ragweed pollen concentration per cubic meter of air;

N is a "mask" that is supposed to be "put up" to each real graph showing the values of experimental data

I is the intensity of the emission of a pollen source.

To formalize the problem, the polar coordinate system was used (Fig.2).

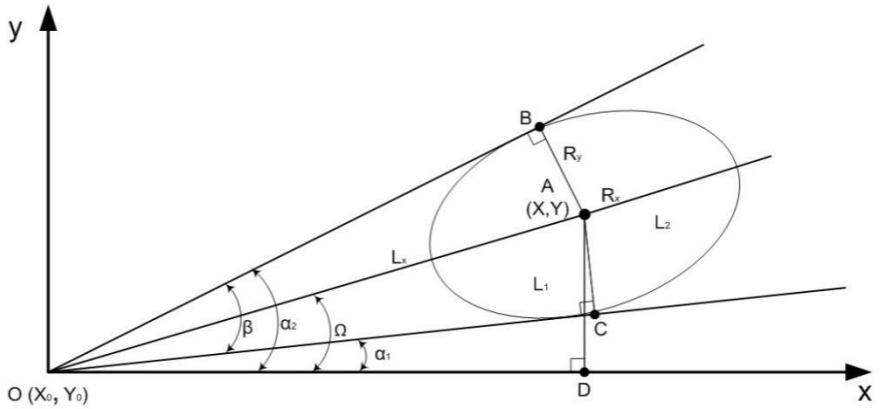

Fig.2. The coordinate system and the formalized spatial parameters of the infested area

X, Y - the coordinates of the centre of the ellipse,
R_x - the radius along the bisector of the sector [α_1, α_2];
R_y - the radius along the axis perpendicular to the bisector within the angle $\beta = \alpha_2 - \alpha_1$;
Ω - the angle of inclination of the ellipse
OX - axis (the angle of inclination of the bisector);
S - the area of the ellipse;
I - the intensity of the infested area

The following parameters of each infested area, represented by the ellipse, were considered: the coordinates (*X, Y*) of the center of the ellipse, the radius R_x along the bisector of the sector [α_1, α_2]; the radius R_y along the axis perpendicular to the bisector within the angle $\beta = \alpha_2 - \alpha_1$; the angle of inclination of the ellipse Ω and the axis OX (the angle of inclination of the bisector); the area of the ellipse *S*; the intensity of the infested area *I*. Hereinafter, the infested area means the area covered by Ambrosia plants within the radius of trap performance (up to 30 km according to Predrag Lugonja et al., 2019).

The solution of the problem was carried out in the following stages.

Stage 1. Preparation. Approximation of the typical solution curves in Fig.1 with splines of the first $y_1(x)$ and second $y_2(x)$ orders. Here it is essential that the segments between the points of the experimental curve had the same inclination as the segments in Fig.1. The free component, on the other hand, can and, as a rule, will be different. Then we proposed to determine the distance to the infested area by the shift of the typical curve along the X-axis (the longer the distance the longer is the delay in the arrival of pollen at the monitoring station). By the shift along the Y-axis we proposed to estimate the plant density in a particular area (a higher density causes higher concentrations of pollen in the air).

Naturally, such an approach, especially using splines of the first order and fitting just two points, may produce many false matches. Therefore, we introduced the criterion of selecting the most probable variants of possible locations of pollen emitting areas. To this end, we utilized the number and relevance of the curves in Fig.1. Firstly, the contribution of each curve in Fig.1 described by the corresponding spline was determined including the total area under the curve (Fig.3).

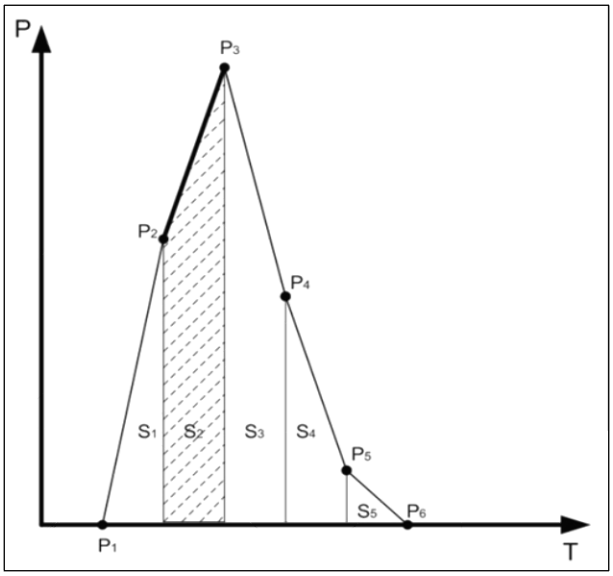

Fig.3 Representation of the process determining the consistency of reliability provided by the second spline of the first order for the segment [P_1, P_2] in the case when the experimental curve is fitted within a given error bound.

For example, for the spline of the type y1(x), the contribution of the *i*-line of the form $y = kx + b$ that connects the points with coordinates (x_i, a_i) and (x_{i-1}, a_{i-1}) ($i = 2, 3, \ldots N_1 = 5$) equals:

$$w_i = \frac{\int_{a_{i-1}}^{a} (kx+b)dx}{\sum_{i=1}^{5} \int_{a_{i-1}}^{a_i} (kx+b)dx}, \quad \int_{a_{i-1}}^{a} (kx+b) = \frac{(a_1-a_2)(2b+a_1k+a_2k)}{2} \; . \qquad (2)$$

The contributions of the two parabolic splines connected in sequence were similarly calculated.

Secondly, performing the approximation of sets of experimental data in each sector over 24-hour intervals, it was analyzed how many splines *M* could be fitted to these sets, and then the probability of the description *D* was calculated as the sum of weights of the corresponding splines:

$$D = \sum_{j=1}^{M} w_j. \quad (3)$$

Thus, the higher the number of the fitted splines, the higher is the reliability of the approximation. If all the splines are fitted, then $D = 1$.

Stage 2: Analysis.

1. In a cycle, we matched the curve in Fig.1 for a certain relative humidity and all the possible sets of sequentially spaced experimental points from each sector in each 24-hour interval to which each of the spline types could be fitted by means of variation of the possible τ-shift (delay). Thus, the time it takes pollen from remote areas to reach and settle on the airborne pollen sampler was determined.

2. In case of a data match, the parameters and probability of location of each possible infested area were calculated.

3. After all possible variants had been searched through, their probability was analyzed. The variants with probability less than 0.45, i.e. those that fit just one curve, were ignored (only one value in case of *RH* = 20% lay above 0.45), but such relative humidity is highly improbable in Ukraine.

4. Then we changed from the polar to the Cartesian coordinate system and constructed ellipses of certain parameters whose color intensity was proportional to their probability.

5. The most likely infested areas are located at the points in which the most ellipses of the highest probability overlap.

The actual fitting of the experimental data to the curves in Fig.1 was performed as follows:

First, it is worth noting that the wind can change direction while pollen grains are carried by the airflow from the emission site toward the monitoring station and, as a result, they may cover a longer distance than they would when moving along a straight line. Thus ideally, it would be recommended to trace the wind trajectory of air masses between the two neighbouring monitoring stations in a given sector – like it is done in Europe but not in Ukraine as the distance between neighboring pollen monitoring sites in the country is at least 240 km. Nevertheless, at the first approximation, we may just include such changes into our calculation, introducing a certain constant h - let's call it a coefficient of graph deformation through changes in wind direction – which is to be multiplied by the current hour at which the experimental data analysis is performed. Hence, the admissible values when analyzing inclinations in Fig.1 are not only $y(x_i - \tau)$ of the typical curve in Fig.1 but also values $y(x_i - \tau \pm hx_i)$. It should also be taken into account that expanding the range of admissible values for all the points of a set means an increase in the range of possible inclinations when checking how closely experimental data match the corresponding spline.

It can be seen from Fig.4 that the whole set of curve inclinations that is possible between all the points on the segments $x_1 \pm h_1$ and $x_2 \pm h_2$ lies between and includes the diagonals BC and AD.

Also, the line BE has the same inclination as AD, ergo the whole set of possible inclinations lies within the triangle BCE, and – as can be easily shown – the inclinations of its sides BC and AD are described by these rather simple equations:

$$k_1 = \frac{dy}{dh+dx+2h_1}, k_2 = -\frac{dy}{dh-dx+2h_1}, dx = x_2 - x_1, dy = y_2 - y_1, dh = h_2 - h_1. \quad (4)$$

We calculated k_1 and k_2 and then determined the minimum and maximum values; thus a set of possible inclinations k for a pair of points of experimental data was determined by such a set within an error bound ε:

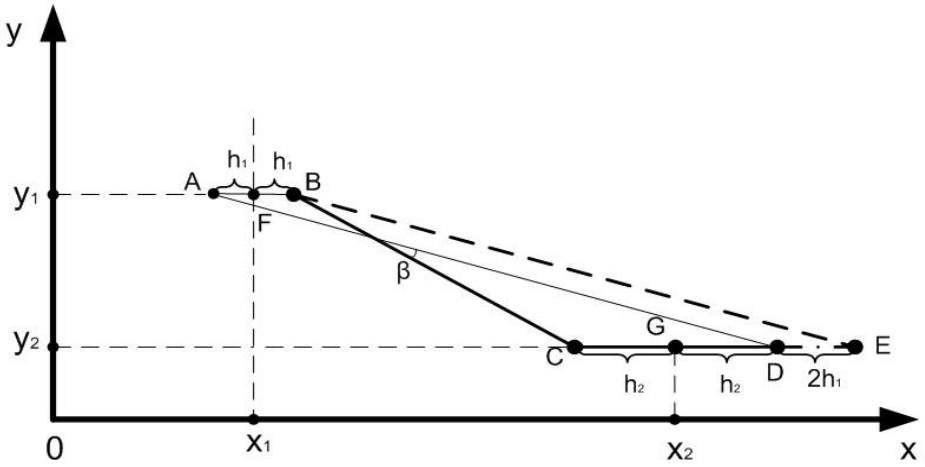

Fig.4 Geometric interpretation of the process of determining a possible set of admissible values for the inclination in the case of the first order spline between a pair of points of experimental data that connects two points $x_1 \pm h_1$ and $x_2 \pm h_2$ with delay $\tau = 0$ including the graph deformation due to a change in wind direction using coefficients h_1 and h_2 correspondingly

To evaluate the parameters of infested areas using Fig.2, it is important to keep in mind that the angles α_1, α_2, β are expressed in degrees or – in calculations with standard computer functions – in radians. However, these angles are also calculated by angles of meteorological data about the wind direction which – as is known – have a different reference point and rotation in the opposite direction. To calculate, for instance, angle α1, the following equation was used:

$$\alpha_1 = (450 - \alpha_{1m})\%\%360 \quad (5)$$

where α_{1m} is meteorological information about the wind direction, degrees; «%%» is an operation that finds the remainder after dividing one number by another (in notation of the R programming language). For example, angle $\alpha_{1m} = 80^0$ yields $\alpha_1 = 10^0$, and angle $\alpha_{1m} = 350^0$ yields $\alpha_1 = 100^0$.

We determined parameters by evaluating the distance to the center of the ellipse along the averaged axis of the wind direction, i.e. the length L_x (in kilometers) of the segment OA:

$$L_x = \gamma v(\tau+1), \quad (6)$$

where γ is a dimensionless coefficient of pollen dispersal that takes into account by how much the speed at which pollen travels is lower than the average wind speed, in the general case, this coefficient is the function of time and space, but at a first approximation it may be considered a constant that, however, should be determined by matching results of field studies of several well-known *Ambrosia* infested areas and their evaluation by this method with an acceptable accuracy;

v is an average wind speed (the mean value of a set of analyzed points), km/h;

τ is the time delay, hours.

As is seen from (6), the center of the infested area is calculated taking into account the distance which pollen grains have covered with a velocity v and time delay τ. The expression $(\tau+1)$ is introduced to allow for the method's limitation in determining the coordinates to the center of an infested area adjacent to the site of the location of the Burkard trap which has the minimum (zero) delay $\tau = 0$. The limitation of this method for Ukraine, as was noted above, is the minimum 2-hour interval of output data. Therefore, the method cannot determine measurements of the nearest infested area more precisely than from 0 to $2\gamma v$, i.e. up to the distance that pollen grains cover in 2 hours. That means that the coordinates of the center cannot be determined with a precision higher than γv, i.e. 1 hour of airborne pollen transport. Similarly, delay τ cannot be determined with a precision higher than $\tau = 2$ hours. Therefore, if $\tau = 0$, the formula (6) should yield the coordinates γv.

We used the dimensions of a ragweed area along the bisector of the sector, i.e. radius Rx, to take into account the indeterminacy of pollen transport dynamics that contains indeterminacy regarding changes in the wind direction (it is evaluated by the maximum additional deformation calculated as the product $(h+1)$ over time $(\tau+1)$ and corresponds to the duration of time that pollen travels from the center of the area), indeterminacy regarding the wind speed (it is evaluated as a difference between the maximum wind speed v_{max} from all the observation points of the set of analyzed values and the average velocity v that is used to calculate distance L_x) and indeterminacy of pollen transport dynamics (evaluated by the coefficient γ):

$$R_x = \gamma(v_{max} - v + v_0)(h+1)(\tau+1) \quad (7)$$

where v_0 is the wind speed that will determine the minimum radius of the ellipse on the graph in the case when the wind speed did not change and the expression $(v_{max} - v)$ equals zero.

The remaining geometric parameters are calculated using the distance L_x and angles α_1, α_2 and β and the known geometric relationships. It was taken into account that the segment AB is perpendicular to segment OB, as follows from the constraint stating that the center of the ellipse is in point A, which is located on the bisector of angle β, and its points lie within the boundaries of the sector limited by angles α_1 and α_2:

$$R_y = \left|L_x \sin\left(\frac{\beta}{2}\right)\right| = \left|L_x \sin\left(\frac{\alpha_2-\alpha_1}{2}\right)\right|, \Omega = \alpha_1 + \beta = \frac{\alpha_1+\alpha_2}{2} \quad (8)$$

$$Y = Y_0 + L_x \sin(\Omega), X = X_0 + L_x \cos(\Omega), S = \pi R_x R_y. \quad (9)$$

It is important to point out that the first two formulas may be presented in a different way depending on the coordinate system which the computer program uses (in many programs the reference point is located in the top left-hand corner of the screen). The presentation of formulas (8,9) corresponds to Fig.2 and the computer program in R which was used to automate this method along with the "Plotrix" library that was used to construct ellipses.

The last of the parameters, intensity I, is determined as a mean calculated by dividing all the experimental data of the set by the values of the typical curves of the graph in Fig.2 at corresponding times with the time delay included:

$$I = \frac{\sum_{i=1}^{M}\left|\frac{y_i(x_i)}{y_1(x_i-\tau)}\right|}{M}. \quad (10)$$

Locations of *Ambrosia* infested areas in Vinnytsia were detected in the course of field studies in 2017 and estimated by the proposed method using the approximation by typical splines of the first order.

Localisation of the ragweed areas following their simulation was carried out by the municipal services of the City of Vinnytsia with their further placement onto the map, which is provided in the Results section.

3 Results:

To automate computations by this method in the R language, the PRA Finder computer program was developed, which has been successfully tested on the real data and for which a certificate of copyright registration has been obtained in Ukraine.

In case of a data match, the parameters and probability of location of each possible infested area were calculated and saved in Table 1.

Table 1. Weights of splines of the first order in description of typical curves in Fig.1

RH, %	90	80	70	60	50	40	30	20
1	0.13	0.09	0.18	0.07	0.24	0.34	0.42	0.56
2	0.36	0.37	0.40	0.35	0.36	0.42	0.33	0.30
3	0.34	0.38	0.32	0.42	0.22	0.19	0.20	0.13
4	0.14	0.13	0.10	0.15	0.13	0.05	0.05	0.01
5	0.03	0.03	0.00	0.01	0.05	0.00	0.00	0.00

The effectiveness of the method has been confirmed using the real data – the known areas were corroborated and new possible plots were revealed. As it was mentioned, locations of *Ambrosia* infested areas in Vinnytsia were detected in the course of field studies in 2017 (dotted lines). They were estimated by the proposed method using the approximation by typical splines of the first order (black lines) for the wind direction from sector [0-120] with error bound ε = 0.01 based on the data for the years 2013 (a) and 2014 (b) (Fig.5).

Fig.5. Results of comparing the locations of *Ambrosia* infested areas in Vinnytsia which were detected during field studies in 2017 (dotted lines) and estimated by the proposed method based on the data for the year a) 2013; b) 2014

Better matches of the real and modeled areas were seen for the results obtained for the year 2014. All the estimated areas matched the real ones. However, it should be taken into consideration that the proposed method is viable only when applied under the conditions when the wind velocity does not exceed 4m/sec and the relative humidity is between 20 % and 90 %. The reason for this is that, at higher wind velocities, the coefficient of graph deformation will be ineffective. In addition, the typical curves in Fig.1 are unknown for the humidity values below 20 % and above 90 %.

Discussion:

The attempt to model ragweed emission sources represented in this study looks successful, especially considering the simulation result obtained for the year 2014 (Fig. 5b). Apparently, the modelling performed for this year was more accurate because the simulation and the field investigation of *Ambrosia* infested areas were closer in time. Thus, simulation was more successful for the year 2014. All the modelled areas matched the real ones and some other ragweed areas were found on site.

Thus, the discrepancy between the modelled and real areas of *Ambrosia* could be explained by a time gap: the pollen count data were collected 3-4 years prior to the simulation. The second possible reason is that pollen monitoring data obtained in the bi-hourly mode have some gaps in the first place: a researcher analyses just 10-12 % of the microscopic sample (Galán, C. et al., 2014). Thus, for the accurate simulation of pollen sources, pollen count from the total area of the slide may be needed. But in practice, when such count is unavailable, the presented method provides the possibility to discover new ragweed areas**.**

Also, it is worth noting that the wind can change direction while pollen grains are carried by airflow from the emission site toward the monitoring station and, as a result, they may cover a longer distance than they would when moving along a straight line (de Weger et. al. 2016). Thus, the actual value should have been registered earlier in the sample whereas in reality it occurred later. What is more, such a discrepancy accumulates – the later in the day pollen grains are detected, the higher the discrepancy is. Thus, as it was mentioned above, wind speed, which exceeds 4 m/s can affect the pollen trajectory, and, consequently, the results of the simulation. This was also taken into account in our model.

We consider that at wind speeds v> 4 m / s the SILAM model (Prank et. al, 2013) becomes more efficient for forecasting than the proposed model. This is expected, because at v = 4.7 m / s per day the pollen passes the distance L = 4.7 m / s × 3.6 km / h × 24 h = 406 km, which corresponds to the distance between the posts of the European Aerobiological Network in Ukraine (Lviv, Odessa, Vinnytsia, Kyiv, Zaporizhia) and pollen counting sites of the neighbouring countries. Thus, localised models show more accurate results at a lower wind speeds.

Approximately the same wind speed as we applied in the current model, which was as low as 4.5km/ h, was used in the model of *Xanthium* pollen distribution by the Chinese authors (Hui L., et al., 2018). It is notable that *Xanthium* is *Ambrosia*'s relative. Both plants belong to the same Asteraceae family. Their pollen has almost the same morphology and both can cause symptoms of pollinosis (Halbritter H. et al. 2018; María Cristina Tellería & Liliana Katinas, 2005).While Martin's model (2010) is applicable for the conditions of relative humidity between 20 % and 90 %, the method is effective in conditions when the average daily relative humidity does not exceed 90 percent. Relative humidity was among the most important meteorological parameters determining the ragweed pollen count in the air along with direction and speed of wind in the research of Stefanic et. al. (2005). Four factors including temperature, wind speed, relative humidity, dew point temperature were retained that explain 84.4% of the total ragweed pollen concentration variance in Southern Hungary (Makra L., Juhász M., 2004). This confirms the importance of inclusion of the relative humidity data into the current simulation.

In spite of some discrepancies between the modelled and real data, the presented case can have the practical significance. First of all, this is because the modelling area, which is limited by the effective radius of Burkard trap performance, is enclosed within the city and adjacent areas. It makes preventive measures more effective as local services can be involved and their efforts may be better coordinated.

What is more, even though *Ambrosia* is one of the three most popular species for model-based forecasting the data about modelling of its spatial distribution and pollen sources are scarce (Maya-Manzano J.M. et al., 2020).

Traditional regression and phenological models (including temperature sum and chilling models) are the most frequently used modelling methods which have been applied to ragweed pollen data in recent years (Maya-Manzano J.M. et al., 2020). However, these models just make it possible to establish and predict the seasonal characteristics of the ragweed regarding the timing

of its pollination, e.g. the start, peak and general progression of the pollen season (Tiffany Duhl. et al., 2013; Shigeto Kawashima et al., 2016).

In addition, in spite of the fact that a number of new modelling techniques have been studied in recent years (Maya-Manzano J.M. et al., 2020; Aurélie Potier et al., 2013), none of them has proposed to use spline interpolation in order to determine the location of pollen sources.

Thus far, most of the methods which aim to determine the spatial distribution of ragweed, as it was mentioned in the Introduction, have usually been applied at the continental or large regional scales (Li Liu et al., 2015; Carsten Ambelas Skjøth et al., 2019).

In the current study, it was important to determine local ragweed infested areas as they can be effectively controlled at a low-scale regional level.

The existing example of modelling pollen distribution at a low scale is the application of the HYSPLYT MODEL to study pollen trajectories across the Andes. (Claudio F. Perez et al., 2009). However, the distance between the pollen emission source and the pollen monitoring site was larger there than in our case.

Thus, in contrast with other known models, which are more often used at the continental and large regional scales (Prank et.al, 2013; Zink et. al, 2012), the described method makes it possible to determine locations of pollen sources within a 30-kilometer radius (Predrag Lugonja et al., 2019) around the Burkard trap. Discrepancy can be explained by the time gap between pollen count data and detection of ragweed infested areas on the ground. The latter was done in 2017, while the pollen count was obtained in 2013 and 2014. However, the simulation can be considered successful while large areas were found.

Synoptic data was taken into consideration for modelling of pollen distribution in a very recent synoptic climatology approach (Anastasia K. Paschalidou et al., 2020).

Conclusions:

1. Spline interpolation is an effective method of detecting location of pollen emission sources at the local level, even in the case when the pollen count data are available only from one site.

2. The method is effective in conditions when the average daily relative humidity does not exceed 90 percent and the wind speed is around 4m/s and less.

3. The efficiency of the method is confirmed by the real data – the known areas were verified and the new possible ragweed infested areas were discovered**.**

Acknowledgments:
The authors would like to thank Aliona Dratsion for editing this article. The authors would like to thank Aliona Dratsion and Tetiana Neprytska, PhD, for editing this article.

References:

Allergenic Pollen. A Review of the Production, Release, Distribution and Health Impacts. Mikhail Sofiev, Karl-Christian Bergmann (2013) , *Springer Science Business Media Dordrecht 2013* https://doi.org/10.1007/978-94-007-4881-1

Anastasia K. Paschalidou, Kyriaki Psistaki, Athanasios Charalampopoulos, Despoina Vokou, Pavlos Kassomenos, Athanasios Damialis (2020). Identifying patterns of airborne pollen distribution using a synoptic climatology approach, *Science of The Total Environment*, Volume 714, 2020, 136625, https://doi.org/10.1016/j.scitotenv.2020.136625

Aurélie Potier, Dmitry Khvorostyanov, Laurent Menut et.al (2013). Modelling birch pollen emission and transport with the chemistry-transport model CHIMERE, April 2013

Carsten Ambelas Skjøth, Yan Sun, Gerhard Karrer, Branko Sikoparija, Matt Smith, Urs Schaffner, Heinz Müller-Schärer (2019). Predicting abundances of invasive ragweed across Europe using a "top-down" approach, *Science of the Total Environment*, 686 (2019) 212-222

Chapman D.S., Makra L., AlbertiniR., Bonini M., Páldy A., Rodinkova V., Šikoparija B., Weryszko-Chmielewska E., Bullock J.M. (2016). Modelling the introduction and spread of non-native species: International trade and climate change drive ragweed invasion. *Global Change Biology*, 22, 3067-3079. doi:10.1111/gcb.13220

Claudio F. Perez, M E Castã Neda, María I Gassmann, María Martha Bianchi (2009). A statistical study of Weinmannia pollen trajectories across the Andes, October 2009, *Advances in Geosciences* 22:79-84

Galán, C., Smith, M., Thibaudon, M., Frenguelli, G., Oteros, J., Gehrig, R., Berger, U., Clot, B., Brandao, R. (2014). Pollen monitoring: minimum requirements and reproducibility of analysis. Aerobiologia. 30, 385-395. https://doi.org/10.1007/s10453-014-9335-5

Halbritter H. et al. (2018) Pollen Morphology and Ultrastructure. In: *Illustrated Pollen Terminology*. *Springer, Cham*. https://doi.org/10.1007/978-3-319-71365-6_3

Hamaoui-Laguel L., Vautard R., Liu L., Solmon F., Viovy N., & Epstein M.M. (2015). Effects of climate change and seed dispersal on airborne ragweed pollen loads in Europe. *Nat Clim Change*, 5: 766–771

Hirst JM (1952) An automatic volumetric spore trap. Ann Appl Biol 39:257–265

Hui L., Mingli Zh., Pengpeng W, Miao M (2018). Study on pollination biology of the invasive plant Xanthium italicum Moretti, *Acta Ecologica Sinica*, 2018 38(5), DOI: 10.5846/stxb201701180158

Li Liu, Fabien Solmon, Robert Vautard, Lynda Hamaoui-Lague, Csaba Zsolt Torma and Filippo Giorgi (2015). Ragweed pollen production and dispersion modelling within a regional climate system, calibration and application over Europe. *Biogeosciences Discussions* 12(21):17595-17641 DOI: 10.5194/bgd-12-17595-2015

Li Liu, Fabien Solmon, Rob ert Vautard et. Al (2016). Ragweed pollen production and dispersion modelling within a regional climate system, calibration and application over Europe, May 2016, *Biogeosciences* 13(9):2769-2786, DOI: 10.5194/bg-13-2769-2016

Letty A. de Weger, Catherine H. Pashley, Branko Šikoparija, Carsten A. Skjøth, Idalia Kasprzyk, Łukasz Grewling, Michel Thibaudon, Donat Magyar & Matt Smith (2016) The long distance transport of airborne Ambrosia pollen to the UK and the Netherlands from Central and south Europe. *International Journal of Biometeorology*, volume 60, pages 1829–1839 https://doi.org/10.1007/s00484-016-1170-7

Makra L., Juhász M (2004). Meteorological variables connected with airborne ragweed pollen in Southern Hungary. *International Journal of Biometeorology* 49(1):37-47, October 2004, https://doi.org/10.1007/s00484-004-0208-4

María Cristina Tellería & Liliana Katinas (2005) The unusual occurrence of tricolpate pollen within Mutisieae (Asteraceae), Grana, 44:2, 91-97, DOI: 10.1080/00173130510010495

Martin M.D., Chamecki M., Brush G.S. (2010). Anthesis synchronization and floral morphology determine diurnal patterns of ragweed pollen dispersal. *Agric. Forest Meteorol*., 150, 1307-1317

Matyasovszky I., Makra L., Tusnády G., Csépe Z., Nyúl L.G., Chapman D.S. (2018). Biogeographical drivers of ragweed pollen concentrations in Europe, *Theor Appl Climatol*, 133 (1-2), 277-295

Maya-Manzano J.M., Smith M., Markey E., Clancy J.H., Sodeau J & O´Connor D. J (2020). Recent developments in monitoring and modelling airborne pollen, *a review*, *Grana* 2020, https://doi.org/10.1080/00173134.2020.1769176

Mokin V.B. (2007) Development of the Geoinformation System of the State Ecological Monitoring. In: Morris A., Kokhan S. (eds) Geographic Uncertainty in Environmental Security. *NATO Science for Peace and Security Series C: Environmental Security*, https://doi.org/10.1007/978-1-4020-6438-8_9

Montagnani C., Gentili R., Smith M., Guarino M. F. & Citterio S. (2017). The Worldwide Spread, Success, and Impact of Ragweed (*Ambrosia spp*.). *Crit Rev Plant Sci*, doi: 10.1080/07352689.2017.1360112

Prank M., Chapman D.S., Bullock J.M., Belmonte J., Berger U., Dahl A. et. al. (2013). An operational model for forecasting ragweed pollen release and dispersion in Europe, *Agric. Forest Meteorol*, 182-183:43-53

Predrag Lugonja, Sanja Brdar, Isidora Simović, Gordan Mimić, Yulii Palamarchuk, Mikhail Sofiev, Branko Šikoparija (2019). Integration of in situ and satellite data for top-down mapping of Ambrosia infection level, *Remote Sensing of Environment*, Volume 235, 15 December 2019,111455 https://doi.org/10.1016/j.rse.2019.111455

Report about the condition of the natural environment of the Vinnytsia region in 2016. (2017). (Доповідь про стан природного середовища у Вінницькій області, 2016 рік). Resource document. Ministry of Ecology and Natural Resources of Ukraine. https://menr.gov.ua/files/docs/Reg.report/%D0%92%D1%96%D0%BD%D0%BD%D0%B8%D1%86%D1%8C%D0%BA%D0%B0_%D0%94%D0%BE%D0%BF_2016.pdf. Accessed 04 April 2021 (in Ukrainian).

Rodinkova V., Palamarchuk O., Toziuk O., Yermishev O. (2018). Modelling hay fever risk factors caused by pollen from Ambrosia spp. using pollen load mapping in Ukraine, *Act Agrobot*, 71 (3): 1742

Rodinkova V.; Yuriev S.; Chopyak V.; Dityatkovaskaya E., Gashinova E., Bezdetko T. et al (2019). Molecular data of pollen sensitization corresponds with pollen spectrum of Ukraine. *Allergy*. 2019; 74 (Suppl. 106): 41, https://doi.org/10.1111/all.13957

Shigeto Kawashima, Satoshi Kobayashi, Keita Tanaka (2016). Modelling of Pollen Emission Process for Dispersal Simulation of Birch Pollen, February 2016, DOI: 10.1007/978-3-319-24478-5_54, In book: *Air Pollution Modelling and its Application XXIV*)

Sikoparija, B., Skjøth, C.A., Celenk, S. et al. Spatial and temporal variations in airborne Ambrosia pollen in Europe. *Aerobiologia 33*, 181–189 (2017). https://doi.org/10.1007/s10453-016-9463-1

Stefanic E, Kovacevic V, Lazanin Z (2005). Airborne ragweed pollen concentration in northeastern Croatia and its relationship with meteorological parameters. *Ann Agric Environ Med*, 12, 75–79 (2005)

Stępalska D., Myszkowska D., Piotrowicz K., Kluska K., Chłopek K., Grewling L., Lafférsová J., Majkowska-Wojciechowska B., Malkiewicz M., Piotrowska-Weryszko K., Puck M., Rodinkova V., Rybníčekm O., Ščevkován J., Voloshchuko K. (2020). High Ambrosia pollen concentrations in Poland respecting the long distance transport (LDT). *Science of The Total Environment Volume 736*, 20 September 2020, 139615, https://doi.org/10.1016/j.scitotenv.2020.139615Get

Stępalska Danuta, (2020). High Ambrosia pollen concentrations in Poland respecting the long distance transport (LDT) б 2020, https://doi.org/10.1016/j.scitotenv.2020.139615 *International Journal of Biometeorology* 60(12) COST Action Review

Tiffany Duhl, Ronson Zhang, Alex B. Guenther, et.al (2013). The Simulator of the Timing and Magnitude of Pollen Season (STaMPS) model: a pollen production model for regional emission and transport modelling, 2013, *Geoscientific Model Development Discussions* 6(6):2325-2368, DOI: 10.5194/gmdd-6-2325-2013

Zink K., Vogel H., Vogel B., Magyar D. & Kottmeier C. (2012). Modelling the dispersion of *Ambrosia* pollen with the model system COSMO-ART. *Int. J. Biometeorol.* 56, 669–680 (2012)